Deterministic generation of qudit photonic graph states from quantum emitters

Zahra Raissi, Edwin Barnes, and Sophia E. Economou
Department of Physics, Virginia Tech, Blacksburg, VA 24061, USA and
Virginia Tech Center for Quantum Information Science and Engineering, Blacksburg, VA 24061, USA

We propose and analyze deterministic protocols to generate qudit photonic graph states from quantum emitters. We exemplify our approach by constructing protocols to generate absolutely maximally entangled states and logical states of quantum error correcting codes. Some of these protocols make use of time-delayed feedback, while others do not. These results significantly broaden the range of multi-photon entangled states that can be produced deterministically from quantum emitters.

I. INTRODUCTION

Entanglement is a uniquely quantum property that plays an important role in almost all aspects of quantum information science, including quantum computing [1], quantum error correction [2, 3], quantum sensing [4], and quantum networks [5–7]. Many of these applications require generating large multi-photon entangled resource states upfront, especially in the context of measurement- or fusion-based quantum computing [8–10] and quantum communication [11–14].

However, creating entangled states of many photons is challenging because photons do not interact directly. Standard ways of circumventing this issue make use of either nonlinear media [15] or quantum interference and measurement [16, 17]; the former approach is made challenging by low coupling efficiencies, while the latter is intrinsically probabilistic. Approaches that rely on interfering photons are usually based on linear optics and post-selection [16, 17], and consequently the success probability decreases exponentially with the number of photons [16, 18]. Despite a number of conceptual and technological advances, the probabilistic nature of this approach continues to severely limit the size of multi-photon entangled states constructed in this way [19, 20].

An alternative approach is to use coupled, controllable quantum emitters with suitable level structures to deterministically generate multi-photon entanglement [21–23]. There now exist several explicit protocols for creating entangled states of many photonic qubits, either by using entangling gates between emitters and transferring entanglement to the photons in the photon emission stage [23–29], or by (re)interfering photons with emitters to create entanglement beyond that potentially generated through the emission process [30–33]. Proof-of-principle experimental demonstrations of such deterministic protocols have been performed in both the optical and microwave domains [34–37].

To date, the vast majority of theoretical and experimental efforts towards the deterministic generation of multi-photon entangled states have focused on photonic qubits. These are based on using either polarization, spatial path, or time bin as the logical encoding. However, photons can naturally encode not only qubits but also multi-dimensional qudit states, for example by using more than two spatial paths or time bins. This can allow for novel approaches to quantum computing, communication, sensing, and error correction in which quantum information is stored in a more compact way [38–40]. Such states can in particular provide benefits in quantum networks and repeaters [41, 42]. Although there have been recent experimental demonstrations of entangled qudit state creation, these have been limited thus far to two photons [38, 43]. An outstanding question is whether multi-photon entangled qudit states can be generated deterministically from a small number of quantum emitters.

In this paper, we propose and evaluate deterministic methods to generate multi-photon qudit graph states from multi-level quantum emitters. We present several different explicit protocols that can produce various states either using a single emitter together with time-delayed feedback, or using multiple coupled quantum emitters. While our approach is quite general, here we focus on constructing highly entangled multipartite states called absolutely maximally entangled (AME) states. These states are defined by the property that they maximize the entanglement entropy for any bipartition [44, 45], and they have applications in quantum error correcting codes (QECCs) and secret sharing [2, 44–50]. In addition, we present protocols for constructing logical states of QECCs whose code spaces are spanned by AME states of qutrits.

The paper is organized as follows. We begin with a brief review of qudit graph states and describe the basic operations needed to create them from quantum emitters (Sec. II). In Sec. III, we describe how to produce photonic qudits from quantum emitters and illustrate our basic approach to multi-qudit-state generation by presenting a protocol to create one-dimensional qudit graph states. In Sec. IV, we present protocols for generating various AME states. Finally, in Sec. V, we show how to generate an explicit example of a QECC whose codewords are all AME states of qutrits. We conclude in Sec. VII.

II. BACKGROUND: QUDITS AND GRAPH STATES

In this work, we focus on the generation of an important class of entangled states called graph states [51]. Graph states are pure quantum states that are defined based on a graph $G = (V, \Gamma)$, which is composed of a set V of n vertices (each qudit is represented by a vertex), and a set of edges specified by the adjacency matrix Γ. Γ is an $n \times n$ symmetric matrix such that $\Gamma_{i,j} = 0$ if vertices i and j are not connected and $\Gamma_{i,j} > 0$ otherwise [51–54]. These states have many applications in measurement-based quantum computing [9, 55], quantum networks [12–14], and QECCs [56, 57].

There are differences between qubit and qudit graph states. For the qubit case, the graph state is defined by initializing all qubits in the $+1$ eigenstate of the X Pauli matrix, i.e., the state $|+\rangle = |0\rangle + |1\rangle$ (here and in the following we will not always explicitly normalize states for the sake of a more compact notation), and then applying controlled-Z (CZ) gates on all pairs of qubits connected by an edge. In the case of qubits, the adjacency matrix Γ contains two different elements: $\Gamma_{i,j} = 0$ whenever two vertices i and j are not connected, and $\Gamma_{i,j} = 1$ otherwise. Most of the existing protocols for creating multi-photon entangled states have focused on the generation of multi-qubit graph states [22–29, 31–33].

To define qudit graph states, we first introduce generalized Pauli operators acting on qudits with q levels [54]. The Pauli operators X and Z act on the eigenstates of Z as follows:

$$X|i\rangle = |i+1 \mod q\rangle, \tag{1}$$
$$Z|i\rangle = \omega^i \, |i\rangle \, . \tag{2}$$

These operators are unitary and traceless, and they satisfy the condition $ZX = \omega XZ$, where $\omega = \mathrm{e}^{\mathrm{i}\,2\pi/q}$ is a q-th root of unity. Each of the Pauli matrices has q eigenvalues and eigenvectors. The powers of X and Z applied to basis states give

$$X^\alpha|i\rangle = |i+\alpha \mod q\rangle, \tag{3}$$
$$Z^\beta|i\rangle = \omega^{i\beta} \, |i\rangle \, , \tag{4}$$

and $X^q = Z^q = \mathbb{1}$. Similar to the case of qubits, we can define controlled-Z^β (CZ^β) gates as

$$CZ^\beta|i,j\rangle = \omega^{\beta\, ij}|i,j\rangle, \qquad \forall \beta \in \{1,\ldots,q-1\} \, . \tag{5}$$

The special case of $q = 2$ in the above corresponds to qubits.

One other operator that is essential to studying qudit graph states is the Hadamard gate. The Hadamard gate H is a matrix that maps the Z-eigenbasis into the X-eigenbasis. For qubits, we have $H|0\rangle = |+\rangle$, and $H|1\rangle = |-\rangle$, where $|-\rangle$ is the -1 eigenvector of the X Pauli operator. There is also a useful identity involving the Hadamard and the Pauli matrices X and Z: $HXH = Z$.

Similarly to the qubit case, we can define the qudit Hadamard operator H such that $H|i\rangle = |X_i\rangle$, where $|X_i\rangle$ is an eigenstate of X. In general, we can write

$$H|i\rangle = \sum_{j=0}^{q-1} \omega^{ij}|j\rangle = |X_i\rangle \qquad \forall i \in \{0,1,...,q-1\} \, . \tag{6}$$

The relationship between the Hadamard and the Pauli operators X^α and Z^α in the case of qudits takes the form

$$HX^\alpha H^\dagger = Z^\alpha, \tag{7}$$

where $H^\dagger$ is the inverse of H:

$$H^\dagger|i\rangle = \sum_{j=0}^{q-1} \omega^{(q-1)ij}|j\rangle = |X_{q-i \bmod q}\rangle, \quad i = 0,...,q-1 \tag{8}$$

Also note that $H^\dagger$ acts on the X-eigenbasis as $H^\dagger|X_i\rangle = |i\rangle$.

To understand how we can use these ingredients to define qudit graph states, we present an explicit example involving qutrits. A qutrit is realized by a 3-level quantum system ($q = 3$), where we denote the Z-eigenstates by $|0\rangle$, $|1\rangle$, and $|2\rangle$. The X-eigenstates then are

$$|X_0\rangle = |0\rangle + |1\rangle + |2\rangle, \tag{9}$$
$$|X_1\rangle = |0\rangle + \omega|1\rangle + \omega^2|2\rangle, \tag{10}$$
$$|X_2\rangle = |0\rangle + \omega^2|1\rangle + \omega|2\rangle \, , \tag{11}$$

where $\omega = e^{\mathrm{i}\,2\pi/3}$. The X operator couples levels as follows: $X|i\rangle = |i+1 \mod 3\rangle$ and $X^2|i\rangle = |i+2 \mod 3\rangle$. The Z and Z^2 operators add different phase factors to each basis state, i.e., $Z|i\rangle = \omega^i|i\rangle$ and $Z^2|i\rangle = \omega^{2i}|i\rangle$, while $X^3 = \mathbb{1}$ and $Z^3 = \mathbb{1}$.

In order to obtain qutrit graph states, we first initialize all qutrits in state $|X_0\rangle$. For each edge, we can consider two possible gates on the corresponding qutrits: CZ and CZ^2, which are defined such that

$$CZ|i,j\rangle = \omega^{ij}|i,j\rangle, \tag{12}$$
$$CZ^2|i,j\rangle = \omega^{2\,ij}|i,j\rangle, \tag{13}$$

where $i,j \in \{0,1,2\}$. Therefore, the adjacency matrix Γ contains three different elements, $\Gamma_{i,j} = 0$ when the two vertices i and j are not connected, $\Gamma_{i,j} = 1$ when they are connected via CZ, and $\Gamma_{i,j} = 2$ when they are connected via CZ^2.

III. EMITTING PHOTONIC QUDITS AND LINEAR GRAPH STATES

In addition to qudit operations, another key ingredient we need to generate qudit photonic graph states is a "pumping" operation that produces photonic qudits from quantum emitters. In this section, we explain how such operations can be realized in systems containing multi-level emitters with the appropriate level structure and selection rules. Later on in Sec. VI, we give explicit examples of such systems, which include color centers in solids and trapped ions. In the present section, we also illustrate how photon pumping, together with qudit operations on emitters and photons, can be used to deterministically create entanglement between photonic qudits.

As a warm-up example illustrating how this works, in this section we present protocols for generating one-dimensional (1D) qudit graph states using a single quantum emitter with an appropriate level structure. This example is closely related to Ref. [58], which showed how to produce a qubit 1D graph state from an emitter comprised of a single electron spin in an optically active quantum dot. That work introduced a protocol in which each photon emission is preceded by a Hadamard gate. Repeating the basic sequence of Hadamard gate followed by optical pumping/photon emission n times results in a n-qubit linear graph state. Because each photon emission can be viewed as a $CNOT$ gate acting on the emitter and emitted photon, this operation together with the Hadamard gates effectively generates the requisite CZ gate between neighboring photonic qubits.

Although the original proposal of Ref. [58] focused on using photon polarization as the qubit degree of freedom, it is important to note that one can also generate a linear graph state based on time-bin qubits by using circularly (rather than linearly) polarized light to pump the emitter and by including a few additional operations during each cycle of the protocol [59]. In this protocol, only one of the emitter ground states, say $|0\rangle_{\rm e}$, can be optically excited by the pump, so that an initial superposition state $|0\rangle_{\rm e}+|1\rangle_{\rm e}$ becomes $|0\rangle_{\rm e}|0\rangle_{\rm p}+|1\rangle_{\rm e}|{\rm vac}\rangle$ after the first photon emission, where $|0\rangle_{\rm p}$ corresponds to a photon in the first time bin, while $|{\rm vac}\rangle$ represents the vacuum. If we then apply an X gate on the emitter and perform a second optical pumping operation, we obtain $|1\rangle_{\rm e}|0\rangle_{\rm p}+|0\rangle_{\rm e}|1\rangle_{\rm p}$, where $|1\rangle_{\rm p}$ corresponds to a photon in the second time bin.

The above protocol for time-bin qubits naturally extends to time-bin qudits with local dimension q, provided we have at our disposal a quantum emitter with q energy levels comprising the ground state manifold, one of which is optically coupled to an excited state. As in the qubit case, upon emission these photonic time-bin qudits will be entangled with the emitter. In general, the cyclic transitions commonly used for optical readout of various qudit systems can be used to optically pump photonic time-bin qudits with q levels through a straightforward generalization of the pumping procedure described above for qubits. For example, consider a three-level quantum emitter with states $|0\rangle_{\rm e}$, $|1\rangle_{\rm e}$, $|2\rangle_{\rm e}$. By starting from an initial equal superposition state $|0\rangle_{\rm e}+|1\rangle_{\rm e}+|2\rangle_{\rm e}$ and interspersing three such pumping/emission events by gate operations that rotate the three different emitter ground states into one another, one can obtain the state $|0\rangle_{\rm e}|0\rangle_{\rm p}+|1\rangle_{\rm e}|1\rangle_{\rm p}+|2\rangle_{\rm e}|2\rangle_{\rm p}$, where $|0\rangle_{\rm p}$, $|1\rangle_{\rm p}$, $|2\rangle_{\rm p}$ are three different photonic time-bin states. We denote this net photon-pumping operation by

$$\mathcal{P}_{\rm pump}(|0\rangle_{\rm e}+|1\rangle_{\rm e}+|2\rangle_{\rm e})=|0\rangle_{\rm e}|0\rangle_{\rm p}+|1\rangle_{\rm e}|1\rangle_{\rm p}+|2\rangle_{\rm e}|2\rangle_{\rm p}. \tag{14}$$

This operation (and its natural generalization to q time bins) is a central ingredient in the protocols that follow.

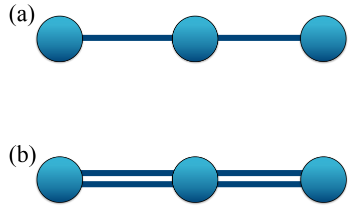

FIG. 1: One-dimensional linear graph states of three qutrits. (a) A linear graph state in which both edges correspond to CZ gates. (b) A linear graph state in which both edges correspond to CZ^2 gates.

Focusing on the qutrit case for concreteness, we now show how to produce linear graph states using Eq. (14). In addition to this photon-pumping operation, we also need to use the qutrit Hadamard operator H in order to obtain the desired entanglement structure in the final multi-photon state. Unlike in the qubit case, in the case of qutrits there are multiple types of linear graph states, depending on whether we use CZ or CZ^2 for each edge. For example, two different linear graph states of three qutrits are shown in Fig. 1, where we use single edges to denote CZ and double edges to denote CZ^2. We can of course also have graph states that contain both types of edges.

With these ingredients in hand, our proposal for generating 1D linear photonic qutrit graph states comprised of only CZ edges (as in Fig. 1(a)) from a quantum emitter with three ground levels is as follows:

1. Prepare the emitter in the state $|0\rangle_{\rm e}$.

2. Perform a Hadamard gate H, Eq. (6), to produce the state $|X_0\rangle=|0\rangle_{\rm e}+|1\rangle_{\rm e}+|2\rangle_{\rm e}$.

3. Generate a time-bin encoded photon with a photon-pumping operation $\mathcal{P}_{\rm pump}$, Eq. (14), to obtain the state $\sum_{i=0}^{2}|i\rangle_{\rm e}|i\rangle_{{\rm p}_1}=|0\rangle_{\rm e}|0\rangle_{{\rm p}_1}+|1\rangle_{\rm e}|1\rangle_{{\rm p}_1}+|2\rangle_{\rm e}|2\rangle_{{\rm p}_1}$.

4. Perform an H gate on the emitter to obtain $\sum_{i,j=0}^{2}\omega^{ij}|j\rangle_{\rm e}|i\rangle_{{\rm p}_1}=|X_0\rangle_{\rm e}|0\rangle_{{\rm p}_1}+|X_1\rangle_{\rm e}|1\rangle_{{\rm p}_1}+|X_2\rangle_{\rm e}|2\rangle_{{\rm p}_1}$.

5. Repeat steps 3 and 4 two more times to produce the state $\sum_{i,j,k,l=0}^{2}\omega^{ij}\omega^{jk}\omega^{kl}\,|l\rangle_{\rm e}|k\rangle_{{\rm p}_3}|j\rangle_{{\rm p}_2}|i\rangle_{{\rm p}_1}$.

6. Measure the emitter in the Z basis to decouple it from the photons. If the measurement

outcome is 0, we obtain the photonic state $\sum_{i,j,k=0}^{2}\omega^{ij}\omega^{jk}\,|k\rangle_{\mathrm{p}_3}|j\rangle_{\mathrm{p}_2}|i\rangle_{\mathrm{p}_1}$, and if the outcome is 1 (or 2), then performing a Z^2 (or Z) gate on photon 3 yields the same photonic state.

The final state is a 3-qutrit linear photonic graph state in which each edge corresponds to a CZ operator, as in Fig. 1(a). By repeating steps 3 and 4 a total of n times, one can produce a linear graph state of n photonic qutrits.

How can we produce a state like that shown in Fig. 1(b)? In this state, each edge now corresponds to a CZ^2 gate. This state can be generated using a very similar protocol as the one above, except that we replace all but the first Hadamard gate by $H^\dagger$ gates:

1. Prepare the emitter in the state $|0\rangle_{\mathrm{e}}$.

2. Perform a Hadamard gate H, Eq. (6), to produce the state $|X_0\rangle = |0\rangle_{\mathrm{e}} + |1\rangle_{\mathrm{e}} + |2\rangle_{\mathrm{e}}$.

3. Generate a time-bin encoded photon with a photon-pumping operation $\mathcal{P}_{\mathrm{pump}}$, Eq. (14), to obtain the state $\sum_{i=0}^{2}|i\rangle_{\mathrm{e}}|i\rangle_{\mathrm{p}_1} = |0\rangle_{\mathrm{e}}|0\rangle_{\mathrm{p}_1} + |1\rangle_{\mathrm{e}}|1\rangle_{\mathrm{p}_1} + |2\rangle_{\mathrm{e}}|2\rangle_{\mathrm{p}_1}$.

4. Perform an $H^\dagger$ gate, Eq. (8), on the emitter to obtain $\sum_{i,j=0}^{2}\omega^{2ij}|j\rangle_{\mathrm{e}}|i\rangle_{\mathrm{p}_1} = |X_0\rangle_{\mathrm{e}}|0\rangle_{\mathrm{p}_1} + |X_2\rangle_{\mathrm{e}}|1\rangle_{\mathrm{p}_1} + |X_1\rangle_{\mathrm{e}}|2\rangle_{\mathrm{p}_1}$.

5. Repeat steps 3 and 4 two more times to produce the state $\sum_{i,j,k,l=0}^{2}\omega^{2ij}\omega^{2jk}\omega^{2kl}\,|l\rangle_{\mathrm{e}}|k\rangle_{\mathrm{p}_3}|j\rangle_{\mathrm{p}_2}|i\rangle_{\mathrm{p}_1}$.

6. Measure the emitter in the Z basis to decouple it from the photons. If the measurement outcome is 0, we obtain the photonic state $\sum_{i,j,k=0}^{2}\omega^{2ij}\omega^{2jk}\,|k\rangle_{\mathrm{e}}|j\rangle_{\mathrm{p}_2}|i\rangle_{\mathrm{p}_1}$, and if the outcome is 1 (or 2), then performing a Z (Z^2) gate on photon 3 yields the same photonic state.

The final state in step 6 is a 3-photonic-qutrit linear graph state with CZ^2 edges, as in Fig. 1(b). Here also, repeating steps 3 and 4 a total of n times yields an n-photon linear graph state with the same structure. Both of the above protocols can be straightforwardly generalized to the case of q-state photonic time-bin graph states generated from q-level quantum emitters.

IV. AME STATE GENERATION

Absolutely maximally entangled (AME) states, also referred to in some works as maximally multipartite entangled states [60–62], are pure n-qudit quantum states with local dimension q such that every reduced density matrix on at most half the system size is maximally mixed. For example, the Bell state $|\phi^+\rangle = |00\rangle + |11\rangle$ and the GHZ state $|GHZ\rangle = |0000\rangle + |1111\rangle$ are both AME states because the reduced density matrices on each half of the system are completely mixed. More formally, an AME(n,q) state is a n-qudit pure state in $\mathcal{H}(n,q) := \mathbb{C}_q^{\otimes n}$ iff

$$\rho_S = \mathrm{Tr}_{S^c}\,|\psi\rangle\langle\psi| \propto \mathbb{1} \qquad \forall S\subset\{1,\ldots,n\}, |S|\leq\lfloor n/2\rfloor\ ,$$

where S^c denotes the complementary set of S. We denote an AME state by $|\mathrm{AME}(n,q)\rangle$. In this section, we describe how one can generate some of these states from quantum emitters.

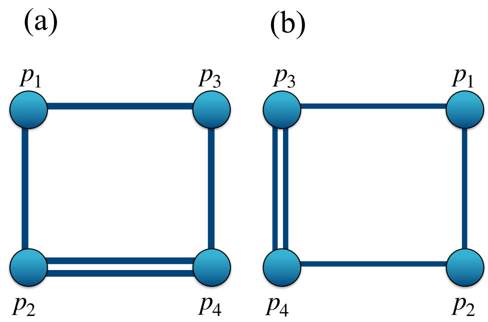

FIG. 2: AME state of 4 qutrits. (a) The graph that represents an AME(4, 3) state. (b) A graph representing a state that is the same as the one in (a) up to a rearrangement of the qutrits.

A. Generating AME states of 4 qutrits

While it is known that AME states of 4 qubits do not exist [2, 63], such states can exist for $q > 2$ [46, 64]. For example, in the case of 4 qutrits ($q = 3$), the corresponding AME state can be written explicitly as [64]:

$$|\mathrm{AME}(4,3)\rangle = \sum_{i,j=0}^{2}|i,j,i+j,i+2j\rangle\ . \tag{15}$$

This state is equivalent to the graph state representation shown in Fig. 2 [64]. In what follows, we present two protocols for generating this state from two quantum emitters, each of which has three ground levels, one of which is optically coupled to an excited state via a cyclic transition. The two protocols produce two states that are the same up to a swapping of two photonic qutrits. The gates we use in the first method (Fig. 2 (a)) are CZ (Eq. (12)), H (Eq. (6)), and $H^\dagger$ (Eq. (8)), and the gates we use in the second method (Fig. 2 (b)) are CZ (Eq. (12)), H (Eq. (6)), and CZ^2 (Eq. (13)). In both protocols, we make use of entangling operations between the emitters, in the spirit of Refs. [24, 27, 29, 65–68].

Here is the first method of generating an AME state of 4 qutrits:

1. Prepare the two emitters in the state $|0\rangle_{\mathrm{e}_1}|0\rangle_{\mathrm{e}_2}$.

2. Perform a Hadamard gate H, Eq. (6), on each emitter to obtain the state $|X_0\rangle_{\mathrm{e}_1}|X_0\rangle_{\mathrm{e}_2} = \sum_{i,j=0}^{2} |i\rangle_{\mathrm{e}_1}|j\rangle_{\mathrm{e}_2}$.
3. Perform a CZ gate, Eq. (12), on the two emitters to obtain $\sum_{i,j=0}^{2} \omega^{ij}\ |i\rangle_{\mathrm{e}_1}|j\rangle_{\mathrm{e}_2}$.
4. Perform photon-pumping operations $\mathcal{P}_{\mathrm{pump}}$, Eq. (14), on each emitter to produce time-bin encoded photons, yielding the state $\sum_{i,j=0}^{2} \omega^{ij}\ |i\rangle_{\mathrm{e}_1}|i\rangle_{\mathrm{p}_1}|j\rangle_{\mathrm{e}_2}|j\rangle_{\mathrm{p}_2}$.
5. Perform an H gate, Eq. (6), on the first emitter and an $H^\dagger$ gate, Eq. (8), on the second emitter to obtain $\sum_{i,j=0}^{2} \omega^{ij}|X_i\rangle_{\mathrm{e}_1}|i\rangle_{\mathrm{p}_1}|X_{2j \bmod 3}\rangle_{\mathrm{e}_2}|j\rangle_{\mathrm{p}_2} = \sum_{i,j,k,l=0}^{2} \omega^{ij}\omega^{ik}\omega^{2jl}\ |k\rangle_{\mathrm{e}_1}|i\rangle_{\mathrm{p}_1}|l\rangle_{\mathrm{e}_2}|j\rangle_{\mathrm{p}_2}$.
6. Perform a CZ gate on the two emitters to produce the state $\sum_{i,j,k,l=0}^{2} \omega^{ij}\omega^{ik}\omega^{2jl}\omega^{kl}\ |k\rangle_{\mathrm{e}_1}|i\rangle_{\mathrm{p}_1}|l\rangle_{\mathrm{e}_2}|j\rangle_{\mathrm{p}_2}$.
7. Perform photon-pumping operations $\mathcal{P}_{\mathrm{pump}}$ on each emitter to produce two more time-bin encoded photons, yielding the state $\sum_{i,j,k,l=0}^{2} \omega^{ij}\omega^{ik}\omega^{2jl}\omega^{kl}\ |k\rangle_{\mathrm{e}_1}|k\rangle_{\mathrm{p}_3}|i\rangle_{\mathrm{p}_1}|l\rangle_{\mathrm{e}_2}|l\rangle_{\mathrm{p}_4}|j\rangle_{\mathrm{p}_2}$.
8. Perform an H gate on each emitter and then measure each emitter in the Z basis. Perform the local gates $Z_{\mathrm{p}_3}^{2o_1} Z_{\mathrm{p}_4}^{2o_2}$ on photons 3 and 4, where o_1 and o_2 are the measurement outcomes for emitters 1 and 2, respectively, to finally arrive at the state $\sum_{i,j,k,l=0}^{2} \omega^{ij}\omega^{ik}\omega^{2jl}\omega^{kl}\ |k\rangle_{\mathrm{p}_3}|i\rangle_{\mathrm{p}_1}|l\rangle_{\mathrm{p}_4}|j\rangle_{\mathrm{p}_2}$.

The final state in step 8 is the state $|\mathrm{AME}(4,3)\rangle$ shown in Fig. 2(a). This state is equivalent to Eq. (15); it can be obtained from that equation by applying Hadamard gates to the third and fourth qudits and by relabeling qutrits.

To produce the state shown in Fig. 2(b), we propose the following slightly modified protocol. The first 4 steps remain the same as above, but steps 5-8 are different:

5. Perform a Hadamard gate H, Eq. (6), on each emitter to obtain the state $\sum_{i,j=0}^{2} \omega^{ij}\ |X_i\rangle_{\mathrm{e}_1}|i\rangle_{\mathrm{p}_1}|X_j\rangle_{\mathrm{e}_2}|j\rangle_{\mathrm{p}_2} = \sum_{i,j,k,l=0}^{2} \omega^{ij}\omega^{ik}\omega^{jl}\ |k\rangle_{\mathrm{e}_1}|i\rangle_{\mathrm{p}_1}|l\rangle_{\mathrm{e}_2}|j\rangle_{\mathrm{p}_2}$.
6. Perform CZ^2, Eq. (13), on the two emitters, after which the state is $\sum_{i,j,k,l=0}^{2} \omega^{ij}\omega^{ik}\omega^{jl}\omega^{2kl}\ |k\rangle_{\mathrm{e}_1}|i\rangle_{\mathrm{p}_1}|l\rangle_{\mathrm{e}_2}|j\rangle_{\mathrm{p}_2}$.
7. Perform photon-pumping operations $\mathcal{P}_{\mathrm{pump}}$, Eq. (14), on each emitter to produce two more time-bin encoded photons, yielding the state $\sum_{i,j,k,l=0}^{2} \omega^{ij}\omega^{ik}\omega^{jl}\omega^{2kl}\ |k\rangle_{\mathrm{e}_1}|k\rangle_{\mathrm{p}_3}|i\rangle_{\mathrm{p}_1}|l\rangle_{\mathrm{e}_2}|l\rangle_{\mathrm{p}_4}|j\rangle_{\mathrm{p}_2}$.
8. Perform an H gate on each emitter and then measure each emitter in the Z basis. Perform the local gates $Z_{\mathrm{p}_3}^{2o_1} Z_{\mathrm{p}_4}^{2o_2}$ on photons 3 and 4, where o_1 and o_2 are the measurement outcomes for emitters 1 and 2, respectively, to finally arrive at the state $\sum_{i,j,k,l=0}^{2} \omega^{ij}\omega^{ik}\omega^{jl}\omega^{2kl}\ |k\rangle_{\mathrm{p}_3}|i\rangle_{\mathrm{p}_1}|l\rangle_{\mathrm{p}_4}|j\rangle_{\mathrm{p}_2}$.

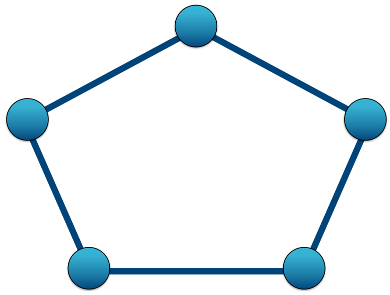

FIG. 3: Graph representation of $\mathrm{AME}(5,q)$ states.

The final state in step 8 is the state shown in Fig. 2(b). We see that we have the freedom to choose between performing a CZ^2 gate on the emitters or performing an $H^\dagger$ (instead of H) gate on one emitter followed by a CZ gate on the two emitters. Note also that larger ladder-type qudit graph states with arbitrary combinations of CZ and CZ^2 edges can be produced by repeating steps 3-6 in the above protocols.

B. Generating AME states of 5 qudits

AME states of 5 qubits were shown to exist in Ref. [69]. By exploiting a connection to quantum orthogonal arrays, explicit examples of $\mathrm{AME}(5,q)$ states for any local dimension $q \geq 2$ were discovered more recently [47]:

$$|\mathrm{AME}(5,q)\rangle = \sum_{i,j=0}^{q-1} |i,j,i+j\rangle|\phi_{i,j}\rangle\ , \qquad (16)$$

where $|\phi_{i,j}\rangle = X^i \otimes Z^j \sum_{\alpha=0}^{q-1} |\alpha,\alpha\rangle$. One can also show that this state has a graph representation. In particular, if one performs Hadamard gates on the third and fourth qudits, the resulting state is the graph state shown in Fig. 3.

In this section we present two general protocols for generating such states that work for all values of the local dimension q. The first uses only a single quantum emitter but assumes the capability of re-interfering an emitted photon with the emitter. The second protocol does not require photon-emitter interference, but at the expense of needing two coupled quantum emitters. In both protocols, we assume the emitters have q ground states, one of which can be optically excited to a higher-energy state via a cyclic transition. This allows for a photon-pumping operation analogous to Eq. (14).

We begin by presenting the protocol that requires only one quantum emitter with q ground levels:

1. Prepare the emitter in the state $|0\rangle_{\mathrm{e}}$.
2. Perform a Hadamard gate H, Eq. (6), to produce the state $|X_0\rangle = \sum_i |i\rangle_{\mathrm{e}}$.

3. Perform a photon-pumping operation $\mathcal{P}_{\text{pump}}$, Eq. (14), to generate a time-bin encoded photon, yielding the state $\sum_{i=0}^{q-1} |i\rangle_{\text{e}}|i\rangle_{\text{p}_1}$.

4. Perform an H gate on the emitter to get $\sum_{i,j=0}^{q-1} \omega^{ij} \, |j\rangle_{\text{e}}|i\rangle_{\text{p}_1}$.

5. Repeat steps 3 and 4 three more times to obtain $\sum_{i,j,k,l,m=0}^{q-1} \omega^{ij}\omega^{jk}\omega^{kl}\omega^{lm} \, |m\rangle_{\text{e}}|l\rangle_{\text{p}_4}|k\rangle_{\text{p}_3}|j\rangle_{\text{p}_2}|i\rangle_{\text{p}_1}$.

6. Interfere the first photon p_1 with the emitter to perform a CZ gate between them, yielding
$$\sum_{i,j,k,l,m} \omega^{ij}\omega^{jk}\omega^{kl}\omega^{lm}\omega^{mi}|m\rangle_{\text{e}}|l\rangle_{\text{p}_4}|k\rangle_{\text{p}_3}|j\rangle_{\text{p}_2}|i\rangle_{\text{p}_1}.$$

7. Perform a photon-pumping operation $\mathcal{P}_{\text{pump}}$ followed by an H gate on the emitter to obtain
$$\sum_{i,j,k,l,m,r} \omega^{ij}\omega^{jk}\omega^{kl}\omega^{lm}\omega^{mi}\omega^{mr}|r\rangle_{\text{e}}|m\rangle_{\text{p}_5}|l\rangle_{\text{p}_4}|k\rangle_{\text{p}_3}|j\rangle_{\text{p}_2}|i\rangle_{\text{p}_1}.$$

8. Measure the emitter in the Z basis and perform $Z_{\text{p}_5}^{(q-1)o}$ on photon p_5, where o is the measurement outcome. The resulting state is the desired AME state:
$$|\text{AME}(5,q)\rangle = \sum_{i,j,k,l,m} \omega^{ij}\omega^{jk}\omega^{kl}\omega^{lm}\omega^{mi}|m\rangle_{\text{p}_5}|l\rangle_{\text{p}_4}|k\rangle_{\text{p}_3}|j\rangle_{\text{p}_2}|i\rangle_{\text{p}_1}.$$

In the protocol described above, we need to re-interfere one of the emitted photons with the emitter to generate a CZ gate between them. While several works have proposed schemes for doing this in the case photonic qubits [31, 32, 70, 71], the analogous qudit operation may be substantially more challenging. This motivates the development of an alternative protocol that does not require such an operation. Such an alternative is possible if have access to two coupled emitters with q ground levels each; one such protocol works as follows:

1. Prepare the two emitters in the state $|0\rangle_{\text{e}_1}|0\rangle_{\text{e}_2}$.

2. Perform a Hadamard gate H, Eq. (6), on each emitter, yielding $\sum_{i,j=0}^{q-1} |i\rangle_{\text{e}_1}|j\rangle_{\text{e}_2}$.

3. Perform a CZ gate, Eq. (5), on the two emitters to get $\sum_{i,j=0}^{q-1} \omega^{ij} \, |i\rangle_{\text{e}_1}|j\rangle_{\text{e}_2}$.

4. Perform photon-pumping operations $\mathcal{P}_{\text{pump}}$, Eq. (14), to each emitter to create two time-bin photonic qudits, yielding $\sum_{i,j=0}^{q-1} \omega^{ij} \, |i\rangle_{\text{e}_1}|i\rangle_{\text{p}_1}|j\rangle_{\text{e}_2}|j\rangle_{\text{p}_2}$.

5. Perform an H gate on each emitter to get $\sum_{i,j,k,l=0}^{q-1} \omega^{ij}\omega^{ik}\omega^{jl} \, |k\rangle_{\text{e}_1}|i\rangle_{\text{p}_1}|l\rangle_{\text{e}_2}|j\rangle_{\text{p}_2}$.

6. Perform a photon-pumping operation on the first emitter (e_1) to produce another photon: $\sum_{i,j,k,l=0}^{q-1} \omega^{ij}\omega^{ik}\omega^{jl} \, |k\rangle_{\text{e}_1}|k\rangle_{\text{p}_3}|i\rangle_{\text{p}_1}|l\rangle_{\text{e}_2}|j\rangle_{\text{p}_2}$.

7. Perform an H gate on the first emitter (e_1) to get $\sum_{i,j,k,l=0}^{q-1} \omega^{ij}\omega^{ik}\omega^{jl}\omega^{km} \, |m\rangle_{\text{e}_1}|k\rangle_{\text{p}_3}|i\rangle_{\text{p}_1}|l\rangle_{\text{e}_2}|j\rangle_{\text{p}_2}$.

8. Perform a CZ gate on the two emitters to get
$$\sum_{\substack{i,j,k,\\ l,m=0}}^{q-1} \omega^{ij}\omega^{ik}\omega^{jl}\omega^{km}\omega^{ml} \, |m\rangle_{\text{e}_1}|k\rangle_{\text{p}_3}|i\rangle_{\text{p}_1}|l\rangle_{\text{e}_2}|j\rangle_{\text{p}_2}.$$

9. Perform a photon-pumping operation on each emitter, followed by an H gate on each emitter:
$$\sum_{\substack{i,j,k,l\\ m,r,s=0}}^{q-1} \Omega|r\rangle_{\text{e}_1}|m\rangle_{\text{p}_4}|k\rangle_{\text{p}_3}|i\rangle_{\text{p}_1}|s\rangle_{\text{e}_2}|l\rangle_{\text{p}_5}|j\rangle_{\text{p}_2},$$
where $\Omega = \omega^{ij}\omega^{ik}\omega^{jl}\omega^{km}\omega^{ml}\omega^{mr}\omega^{ls}$.

10. Measure both emitters in the Z basis and perform $Z_{\text{p}_4}^{(q-1)o_1} Z_{\text{p}_5}^{(q-1)o_2}$ on photons p_4 and p_5, where o_1 and o_2 are the measurement outcomes. This yields the desired 5-photon state:
$$|\text{AME}(5,q)\rangle = \sum_{\substack{i,j,k,\\ l,m=0}}^{q-1} \omega^{ij}\omega^{ik}\omega^{jl}\omega^{km}\omega^{ml} \, |m\rangle_{\text{p}_5}|k\rangle_{\text{p}_3}|i\rangle_{\text{p}_1}|l\rangle_{\text{p}_4}|j\rangle_{\text{p}_2}.$$

C. Generating AME states of 6 qudits

Next, we consider AME$(6,q)$ states. The graph representations of two such states are shown in Fig. 4 [64, 72]. Here, we present protocols for generating both of these types of graph states for qudits of arbitrary local dimension q. The first protocol utilizes two coupled emitters with q ground levels each and photon-emitter interference to generate graph states of the sort shown in Fig. 4(a). The protocol consists of the following steps:

1. Prepare two q-level emitters in the state $|0\rangle_{\text{e}_1}|0\rangle_{\text{e}_2}$.

2. Perform a Hadamard gate H, Eq. (6), on each emitter to obtain $\sum_{i,j=0}^{q-1} |i\rangle_{\text{e}_1}|j\rangle_{\text{e}_2}$.

3. Perform a CZ gate, Eq. (5), on the two emitters to get $\sum_{i,j=0}^{q-1} \omega^{ij} \, |i\rangle_{\text{e}_1}|j\rangle_{\text{e}_2}$.

4. Perform photon-pumping operations $\mathcal{P}_{\text{pump}}$, Eq. (14), on each emitter to produce two photons: $\sum_{i,j=0}^{q-1} \omega^{ij} \, |i\rangle_{\text{e}_1}|i\rangle_{\text{p}_1}|j\rangle_{\text{e}_2}|j\rangle_{\text{p}_2}$.

5. Perform an H gate on each emitter to obtain $\sum_{i,j,k,l=0}^{q-1} \omega^{ij}\omega^{ik}\omega^{jl} \, |k\rangle_{\text{e}_1}|i\rangle_{\text{p}_1}|l\rangle_{\text{e}_2}|j\rangle_{\text{p}_2}$.

6. Apply two CZ gates, one on the first photon (p_1) and the second emitter (e_2), and the other on the two emitters, yielding $\sum_{i,j,k,l=0}^{q-1} \omega^{ij}\omega^{ik}\omega^{jl}\omega^{il}\omega^{kl} \, |k\rangle_{\text{e}_1}|i\rangle_{\text{p}_1}|l\rangle_{\text{e}_2}|j\rangle_{\text{p}_2}$.

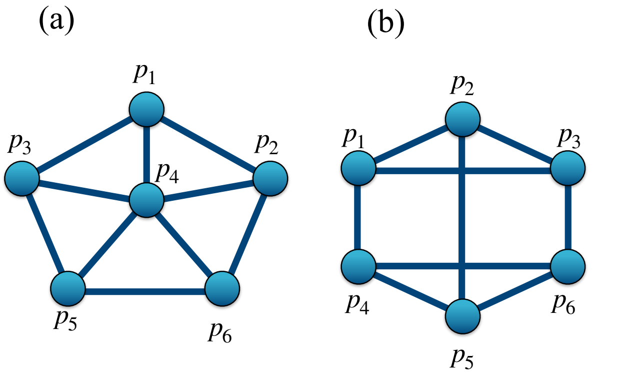

FIG. 4: Two types of AME$(6, q)$ states represented as graphs.

7. Perform photon-pumping operations on each emitter to create two more photons: $\sum_{i,j,k,l} \omega^{ij}\omega^{ik}\omega^{jl}\omega^{il}\omega^{kl} \; |k\rangle_{\mathrm{e}_1}|k\rangle_{\mathrm{p}_3}|i\rangle_{\mathrm{p}_1}|l\rangle_{\mathrm{e}_2}|l\rangle_{\mathrm{p}_4}|j\rangle_{\mathrm{p}_2}$.

8. Perform an H gate on each emitter to get $\sum_{\substack{i,j,k,\\ l,m,r}} \Omega \; |m\rangle_{\mathrm{e}_1}|k\rangle_{\mathrm{p}_3}|i\rangle_{\mathrm{p}_1}|r\rangle_{\mathrm{e}_2}|l\rangle_{\mathrm{p}_4}|j\rangle_{\mathrm{p}_2}$, where $\Omega := \omega^{ij}\omega^{ik}\omega^{jl}\omega^{il}\omega^{kl}\omega^{km}\omega^{lr}$.

9. Perform three CZ gates: One CZ on p_4 and e_1, the other CZ on p_2 and e_2, and the third CZ operator on e_1 and e_2. With this we obtain

$$\sum_{\substack{i,j,k,\\ l,m,r=0}}^{q-1} \Omega' \; |m\rangle_{\mathrm{e}_1}|k\rangle_{\mathrm{p}_3}|i\rangle_{\mathrm{p}_1}|r\rangle_{\mathrm{e}_2}|l\rangle_{\mathrm{p}_4}|j\rangle_{\mathrm{p}_2},$$

where $\Omega' := \omega^{ij}\omega^{ik}\omega^{jl}\omega^{il}\omega^{kl}\omega^{km}\omega^{lr}\omega^{lm}\omega^{jr}\omega^{mr}$.

10. Perform a photon-pumping operation on each emitter, followed by an H gate on each emitter. Measure both emitters and perform the gates $Z_{\mathrm{p}_5}^{(q-1)o_1} Z_{\mathrm{p}_6}^{(q-1)o_2}$ on the newly generated photons p_5 and p_6, where o_1 and o_2 are the measurement outcomes. The final state is

$$|\mathrm{AME}(6, q)\rangle = \sum_{\substack{i,j,k,\\ l,m,r=0}}^{q-1} \Omega' \; |m\rangle_{\mathrm{p}_5}|k\rangle_{\mathrm{p}_3}|i\rangle_{\mathrm{p}_1}|r\rangle_{\mathrm{p}_6}|l\rangle_{\mathrm{p}_4}|j\rangle_{\mathrm{p}_2},$$

which is the one shown in Fig. 4(a).

We now present a protocol for generating the AME$(6, q)$ states corresponding to the graph shown in Fig. 4(b). This protocol requires three coupled emitters with q ground levels each but does not need photon-emitter interference:

1. Prepare three emitters in the state $|0\rangle_{\mathrm{e}_1}|0\rangle_{\mathrm{e}_2}|0\rangle_{\mathrm{e}_3}$.

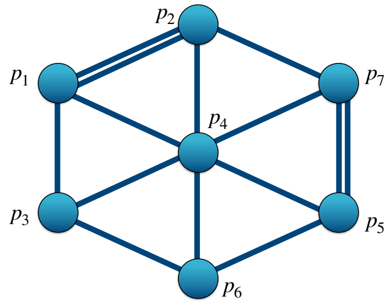

FIG. 5: Graph representing the AME$(7, 3)$ state.

2. Perform a Hadamard gate H, Eq. (6), on each emitter to obtain $\sum_{i,j,k=0}^{q-1} |i\rangle_{\mathrm{e}_1}|j\rangle_{\mathrm{e}_2}|k\rangle_{\mathrm{e}_3}$.

3. Perform three CZ gates on each pair of emitters (i.e., on e_1 and e_2, on e_2 and e_3, and on e_1 and e_3): $\sum_{i,j,k=0}^{q-1} \omega^{ij}\omega^{jk}\omega^{ik} \; |i\rangle_{\mathrm{e}_1}|j\rangle_{\mathrm{e}_2}|k\rangle_{\mathrm{e}_3}$.

4. Perform photon-pumping operations $\mathcal{P}_{\mathrm{pump}}$, Eq. (14), to each emitter to create three photons: $\sum_{i,j,k=0}^{q-1} \omega^{ij}\omega^{jk}\omega^{ik} \; |i\rangle_{\mathrm{e}_1}|i\rangle_{\mathrm{p}_1}|j\rangle_{\mathrm{e}_2}|j\rangle_{\mathrm{p}_2}|k\rangle_{\mathrm{e}_3}|k\rangle_{\mathrm{p}_3}$.

5. Perform an H gate on each emitter: $\sum_{i,j,k,l,m,r=0}^{q-1} \Theta \; |l\rangle_{\mathrm{e}_1}|i\rangle_{\mathrm{p}_1}|m\rangle_{\mathrm{e}_2}|j\rangle_{\mathrm{p}_2}|r\rangle_{\mathrm{e}_3}|k\rangle_{\mathrm{p}_3}$, where $\Theta := \omega^{ij}\omega^{jk}\omega^{ik}\omega^{il}\omega^{jm}\omega^{kr}$.

6. Again perform a CZ gate on each pair of emitters:

$$\sum_{i,j,k,l,m,r=0}^{q-1} \Theta' \; |l\rangle_{\mathrm{e}_1}|i\rangle_{\mathrm{p}_1}|m\rangle_{\mathrm{e}_2}|j\rangle_{\mathrm{p}_2}|r\rangle_{\mathrm{e}_3}|k\rangle_{\mathrm{p}_3},$$

where $\Theta' := \omega^{ij}\omega^{jk}\omega^{ik}\omega^{il}\omega^{jm}\omega^{kr}\omega^{lm}\omega^{mr}\omega^{lr}$.

10. Perform a photon-pumping operation on each emitter, followed by an H gate on each emitter. Measure all three emitters and perform the gates $Z_{\mathrm{p}_4}^{(q-1)o_1} Z_{\mathrm{p}_5}^{(q-1)o_2} Z_{\mathrm{p}_6}^{(q-1)o_3}$ on the newly generated photons p_4, p_5, and p_6, where o_1, o_2, o_3 are the measurement outcomes. The final state is

$$|\mathrm{AME}(6, q)\rangle = \sum_{i,j,k,l,m,r=0}^{q-1} \Theta' \; |l\rangle_{\mathrm{p}_4}|i\rangle_{\mathrm{p}_1}|m\rangle_{\mathrm{p}_5}|j\rangle_{\mathrm{p}_2}|r\rangle_{\mathrm{p}_6}|k\rangle_{\mathrm{p}_3},$$

which is the one shown in Fig. 4(b).

D. Generating AME states of 7 qutrits

It is known that while AME states of 7 qubits do not exist [73], AME states of 7 qutrits do exist. Through an exhaustive numerical search checking the bipartite entanglement of various graph states, it was found that the graph shown in Fig. 5 corresponds to the AME$(7, 3)$ state [64]. In this section, we show how to generate this state. Our protocol uses two quantum emitters with three ground levels each, as well as photon-emitter interference. The protocol is similar to the one presented above for the AME(6,q) states depicted in Fig. 4 due to the similarity in graph structure.

1. Prepare the two quantum emitters in the state $|0\rangle_{\mathrm{e}_1}|0\rangle_{\mathrm{e}_2}$.
2. Perform a Hadamard gate H, Eq. (6), on each emitter: $|X_0\rangle_{\mathrm{e}_1}|X_0\rangle_{\mathrm{e}_2} = \sum_{i,j=0}^{2} |i\rangle_{\mathrm{e}_1}|j\rangle_{\mathrm{e}_2}$.
3. Perform CZ^2, Eq. (13), on the two emitters to get $\sum_{i,j=0}^{2} \omega^{2ij}\ |i\rangle_{\mathrm{e}_1}|j\rangle_{\mathrm{e}_2}$.
4. Perform the photon-pumping operation $\mathcal{P}_{\mathrm{pump}}$, Eq. (14), on each emitter to create two photons: $\sum_{i,j=0}^{2} \omega^{2ij}\ |i\rangle_{\mathrm{e}_1}|i\rangle_{\mathrm{p}_1}|j\rangle_{\mathrm{e}_2}|j\rangle_{\mathrm{p}_2}$.
5. Perform an H gate on each emitter: $\sum_{i,j,k,l=0}^{2} \omega^{2ij}\omega^{ik}\omega^{jl}\ |k\rangle_{\mathrm{e}_1}|i\rangle_{\mathrm{p}_1}|l\rangle_{\mathrm{e}_2}|j\rangle_{\mathrm{p}_2}$.
6. Apply two CZ gates, Eq. (12), one on the first photon (p_1) and the second emitter (e_2), and the other on the two emitters (e_1 and e_2), yielding $\sum_{i,j,k,l=0}^{2} \omega^{2ij}\omega^{ik}\omega^{jl}\omega^{il}\omega^{kl}\ |k\rangle_{\mathrm{e}_1}|i\rangle_{\mathrm{p}_1}|l\rangle_{\mathrm{e}_2}|j\rangle_{\mathrm{p}_2}$.
7. Perform photon-pumping operations on each emitter to create two more photons: $\sum_{\substack{i,j,\\k,l}} \omega^{2ij}\omega^{ik}\omega^{jl}\omega^{il}\omega^{kl}\ |k\rangle_{\mathrm{e}_1}|k\rangle_{\mathrm{p}_3}|i\rangle_{\mathrm{p}_1}|l\rangle_{\mathrm{e}_2}|l\rangle_{\mathrm{p}_4}|j\rangle_{\mathrm{p}_2}$.
8. Perform an H gate on each emitter: $\sum_{\substack{i,j,k,\\l,m,r=0}}^{2} \Xi\ \ |m\rangle_{\mathrm{e}_1}|k\rangle_{\mathrm{p}_3}|i\rangle_{\mathrm{p}_1}|r\rangle_{\mathrm{e}_2}|l\rangle_{\mathrm{p}_4}|j\rangle_{\mathrm{p}_2}$, where $\Xi := \omega^{2ij}\omega^{ik}\omega^{jl}\omega^{il}\omega^{kl}\omega^{km}\omega^{lr}$.
9. Perform two CZ gates, one on p_4 and e_1, the other on e_1 and e_2, yielding $\sum_{\substack{i,j,k,\\l,m,r=0}}^{2} \Xi'\ \ |m\rangle_{\mathrm{e}_1}|k\rangle_{\mathrm{p}_3}|i\rangle_{\mathrm{p}_1}|r\rangle_{\mathrm{e}_2}|l\rangle_{\mathrm{p}_4}|j\rangle_{\mathrm{p}_2}$ where $\Xi' := \omega^{2ij}\omega^{ik}\omega^{jl}\omega^{il}\omega^{kl}\omega^{km}\omega^{lr}\omega^{lm}\omega^{mr}$.
10. Perform a photon-pumping operation on only e_2 to create one more photon: $\sum_{\substack{i,j,k,\\l,m,r=0}}^{2} \Xi'\ |m\rangle_{\mathrm{e}_1}|k\rangle_{\mathrm{p}_3}|i\rangle_{\mathrm{p}_1}|r\rangle_{\mathrm{e}_2}|r\rangle_{\mathrm{p}_5}|l\rangle_{\mathrm{p}_4}|j\rangle_{\mathrm{p}_2}$.
11. Perform an $H^\dagger$ gate, Eq. (8), on e_2 to yield $\sum_{\substack{i,j,k,l\\m,r,s=0}}^{2} \Xi''\ |m\rangle_{\mathrm{e}_1}|k\rangle_{\mathrm{p}_3}|i\rangle_{\mathrm{p}_1}|s\rangle_{\mathrm{e}_2}|r\rangle_{\mathrm{p}_5}|l\rangle_{\mathrm{p}_4}|j\rangle_{\mathrm{p}_2}$ where $\Xi'' := \omega^{2ij}\omega^{ik}\omega^{jl}\omega^{il}\omega^{kl}\omega^{km}\omega^{lr}\omega^{lm}\omega^{mr}\omega^{2sr}$.
12. Apply two CZ gates, one on the fourth photon (p_4) and the second emitter (e_2), and the other on p_2 and e_2:
$$\sum_{\substack{i,j,k,l\\m,r,s=0}}^{2} \tilde{\Xi}\ |m\rangle_{\mathrm{e}_1}|k\rangle_{\mathrm{p}_3}|i\rangle_{\mathrm{p}_1}|s\rangle_{\mathrm{e}_2}|r\rangle_{\mathrm{p}_5}|l\rangle_{\mathrm{p}_4}|j\rangle_{\mathrm{p}_2}.$$
where
$$\tilde{\Xi} := \omega^{2ij}\omega^{ik}\omega^{jl}\omega^{il}\omega^{kl}\omega^{km}\omega^{lr}\omega^{lm}\omega^{mr}\omega^{2sr}\omega^{sl}\omega^{js}.$$
13. Perform a photon-pumping operation on each emitter, followed by an H gate on each emitter. Measure both emitters in the Z basis and perform the gates $Z_{\mathrm{p}_6}^{(q-1)o_1} Z_{\mathrm{p}_7}^{(q-1)o_2}$ on the newly generated photons, p_6 and p_7, where o_1 and o_2 are the measurement outcomes. The final state is
$$|\mathrm{AME}(7,3)\rangle = \sum_{\substack{i,j,k,l\\m,r,s=0}}^{2} \tilde{\Xi}\ |m\rangle_{\mathrm{p}_6}|k\rangle_{\mathrm{p}_3}|i\rangle_{\mathrm{p}_1}|s\rangle_{\mathrm{p}_7}|r\rangle_{\mathrm{p}_5}|l\rangle_{\mathrm{p}_4}|j\rangle_{\mathrm{p}_2},$$
which is the state shown in Fig. 5.

A summary of the multi-qudit graph states generation protocols presented so far is given in Table. I.

V. QUANTUM ERROR CORRECTING CODES

It is known that AME states are useful for constructing QECCs [2, 46, 49]. In this section, we show how this connection can be exploited to develop protocols for generating multiphoton logical states of QECCs. First, we briefly review the relation between certain QECCs and AME states. A subspace $\mathcal{C}$ spanned by an orthonormal set of states $\{|\psi_0\rangle, |\psi_1\rangle, \ldots, |\psi_{q^k-1}\rangle\}$, also called *codewords*, is a QECC with parameters $[\![n,k,d]\!]_q$. This code is a q^k dimensional subspace that encodes k logical qudits into n physical qudits, if it obeys the Knill-Laflamme conditions [56, 74]

$$\forall m, m' \in [q^k]:\ \langle\psi_m|E^\dagger F|\psi_{m'}\rangle = f(E^\dagger F)\,\delta_{m,m'}, \quad (17)$$

for all errors E, F with weight$(E^\dagger F) \le d$, where the weight of an operator is defined to be the number of sites on which it acts non-trivially. The parameter d is the distance of the quantum code, which is the minimal number of single-qudit operations that are needed to create a non-zero overlap between any two codewords from the code state space $\mathcal{C}$. A QECC with minimum distance d can correct errors that affect no more than $(d-1)/2$ of the physical qudits. In this section, we show how to generate a $[\![3,1,2]\!]_3$ QECC, for which the codewords are all AME states of 3 qutrits.

Graph	# photons	Local dimension	# emitters	Photon interference required?
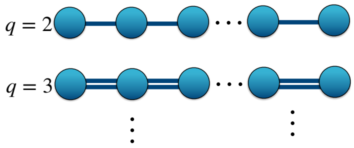	$n \geq 2$	$q \geq 2$	1	no
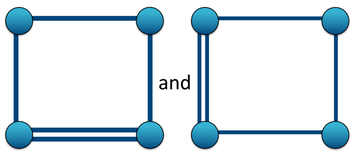	$n = 4$	$q = 3$	2	no
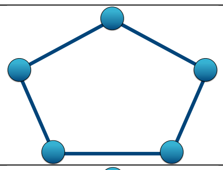	$n = 5$	$q \geq 2$	First method: 1 Second method: 2	yes no
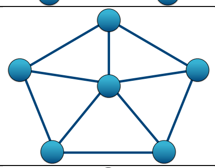	$n = 6$	$q \geq 2$	2	yes
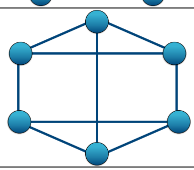	$n = 6$	$q \geq 2$	3	no
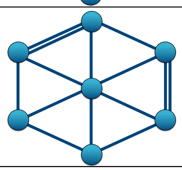	$n = 7$	$q = 3$	2	yes

TABLE I: Summary of the generation protocols of various multi-photon qudit graph states presented in this work. For each protocol, the corrsponding graph representation of the target state is shown, along with the number of photons it contains, the number q of photonic time-bin states, the number of quantum emitters (with q levels each) needed to produce the state, and whether or not photon-emitter interference is required for the protocol.

First, let us review how to construct the $[\![3,1,2]\!]_3$ quantum code (see also [3, 49, 75]). It is known that the AME(3, 3) states [49, 76]

$$\begin{aligned} |\psi_0\rangle &= \sum_{j=0}^{2} |j,j,j\rangle, \\ |\psi_1\rangle &= M|\psi_0\rangle = \sum_{j=0}^{2} |j+1,j,j+2\rangle, \\ |\psi_2\rangle &= M^2|\psi_0\rangle = \sum_{j=0}^{2} |j+2,j,j+1\rangle, \end{aligned} \tag{18}$$

are the codewords of the $[\![3,1,2]\!]_3$ code. In the above, the operator M is defined as $M = X \otimes \mathbb{1} \otimes X^2$.

In order to construct the corresponding graph states, it helps to first notice that by performing an H gate, Eq. (6), on the first and third qudits, we get

$$|\psi_0'\rangle = H \otimes \mathbb{1} \otimes H\,|\psi_0\rangle = \sum_{i,j,k=0}^{2} \omega^{kj}\omega^{ij}\;|k,j,i\rangle, \tag{19}$$

$$|\psi_1'\rangle = H \otimes \mathbb{1} \otimes H\,|\psi_1\rangle = \sum_{i,j,k=0}^{2} \omega^{(j+1)k}\omega^{(j+2)i}\;|k,j,i\rangle, \tag{20}$$

$$|\psi_2'\rangle = H \otimes \mathbb{1} \otimes H\,|\psi_2\rangle = \sum_{i,j,k=0}^{2} \omega^{(j+2)k}\omega^{(j+1)i}\ |k,j,i\rangle\,. \tag{21}$$

Notice that the state $|\psi_0'\rangle$ is equivalent to the 3-qutrit graph state shown in Fig. 1(a) and discussed in Sec. III. Thus, we already know how to generate this state, and so it remains to show how to produce $|\psi_1'\rangle$ and $|\psi_2'\rangle$ from a 3-level quantum emitter. For this, let us first discuss how to generate $|\psi_1'\rangle$:

1. Prepare the emitter in the state $|2\rangle_{\mathrm{e}}$.
2. Perform a Hadamard gate H, Eq. (6), to produce the state $|X_2\rangle_{\mathrm{e}} = \sum_{i=0}^{2}\omega^{2i}|i\rangle_{\mathrm{e}} = |0\rangle_{\mathrm{e}} + \omega^2|1\rangle_{\mathrm{e}} + \omega|2\rangle_{\mathrm{e}}$.
3. Generate a time-bin encoded photon with a photon-pumping operation $\mathcal{P}_{\mathrm{pump}}$, Eq. (14), to obtain the state $\sum_{i=0}^{2}\omega^{2i}|i\rangle_{\mathrm{e}}|i\rangle_{\mathrm{p}_1} = |0\rangle_{\mathrm{e}}|0\rangle_{\mathrm{p}_1} + \omega^2|1\rangle_{\mathrm{e}}|1\rangle_{\mathrm{p}_1} + \omega|2\rangle_{\mathrm{e}}|2\rangle_{\mathrm{p}_1}$.
4. Perform an H gate, Eq. (6), on the emitter to obtain $\sum_{i,j=0}^{2}\omega^{2i}\omega^{ij}|j\rangle_{\mathrm{e}}|i\rangle_{\mathrm{p}_1} = |X_0\rangle_{\mathrm{e}}|0\rangle_{\mathrm{p}_1} + \omega^2|X_1\rangle_{\mathrm{e}}|1\rangle_{\mathrm{p}_1} + \omega|X_2\rangle_{\mathrm{e}}|2\rangle_{\mathrm{p}_1}$.
5. Repeat steps 3 and 4 to produce the state $\sum_{i,j,k=0}^{2}\omega^{2i}\omega^{ij}\omega^{jk}\,|k\rangle_{\mathrm{e}}|j\rangle_{\mathrm{p}_2}|i\rangle_{\mathrm{p}_1}$.
6. Perform a Z gate, Eq. (2), on the emitter to obtain $\sum_{i,j,k=0}^{2}\omega^{2i}\omega^{ij}\omega^{jk}\omega^{k}\,|k\rangle_{\mathrm{e}}|j\rangle_{\mathrm{p}_2}|i\rangle_{\mathrm{p}_1}$.
7. Repeat steps 3 and 4 once more to produce the state $\sum_{i,j,k,l=0}^{2}\omega^{2i}\omega^{ij}\omega^{jk}\omega^{k}\omega^{kl}\,|l\rangle_{\mathrm{e}}|k\rangle_{\mathrm{p}_3}|j\rangle_{\mathrm{p}_2}|i\rangle_{\mathrm{p}_1}$.
8. Measure the emitter in the Z basis and perform the gate $Z_{\mathrm{p}_3}^{2o}$ on photon p_3, where o is the measurement outcome. The resulting state is the desired $|\psi_1'\rangle$:

$$|\psi_1'\rangle = \sum_{i,j,k=0}^{2} \omega^{2i}\omega^{ij}\omega^{jk}\omega^{k}\,|k\rangle_{\mathrm{p}_3}|j\rangle_{\mathrm{p}_2}|i\rangle_{\mathrm{p}_1}\ . \tag{22}$$

A similar protocol can be used to generate $|\psi_2'\rangle$:

1. Prepare the emitter in the state $|1\rangle_{\mathrm{e}}$.
2. Perform a Hadamard gate H, Eq. (6), to produce the state $|X_1\rangle_{\mathrm{e}} = \sum_{i=0}^{2}\omega^{i}|i\rangle_{\mathrm{e}} = |0\rangle_{\mathrm{e}} + \omega|1\rangle_{\mathrm{e}} + \omega^2|2\rangle_{\mathrm{e}}$.
3. Generate a time-bin encoded photon with a photon-pumping operation $\mathcal{P}_{\mathrm{pump}}$, Eq. (14), to obtain the state $\sum_{i=0}^{2}\omega^{i}|i\rangle_{\mathrm{e}}|i\rangle_{\mathrm{p}_1} = |0\rangle_{\mathrm{e}}|0\rangle_{\mathrm{p}_1} + \omega|1\rangle_{\mathrm{e}}|1\rangle_{\mathrm{p}_1} + \omega^2|2\rangle_{\mathrm{e}}|2\rangle_{\mathrm{p}_1}$.
4. Perform an H gate, Eq. (6), on the emitter to obtain $\sum_{i,j=0}^{2}\omega^{i}\omega^{ij}|j\rangle_{\mathrm{e}}|i\rangle_{\mathrm{p}_1} = |X_0\rangle_{\mathrm{e}}|0\rangle_{\mathrm{p}_1} + \omega|X_1\rangle_{\mathrm{e}}|1\rangle_{\mathrm{p}_1} + \omega^2|X_2\rangle_{\mathrm{e}}|2\rangle_{\mathrm{p}_1}$.
5. Repeat steps 3 and 4 to produce the state $\sum_{i,j,k=0}^{2}\omega^{i}\omega^{ij}\omega^{jk}\,|k\rangle_{\mathrm{e}}|j\rangle_{\mathrm{p}_2}|i\rangle_{\mathrm{p}_1}$.
6. Perform a Z^2 gate, Eq. (4), on the emitter to obtain $\sum_{i,j,k=0}^{2}\omega^{i}\omega^{ij}\omega^{jk}\omega^{2k}\,|k\rangle_{\mathrm{e}}|j\rangle_{\mathrm{p}_2}|i\rangle_{\mathrm{p}_1}$.
7. Repeat steps 3 and 4 once more to produce the state $\sum_{i,j,k,l=0}^{2}\omega^{i}\omega^{ij}\omega^{jk}\omega^{2k}\omega^{kl}\,|l\rangle_{\mathrm{e}}|k\rangle_{\mathrm{p}_3}|j\rangle_{\mathrm{p}_2}|i\rangle_{\mathrm{p}_1}$.
8. Measure the emitter in the Z basis and perform the gate $Z_{\mathrm{p}_3}^{2o}$ on photon p_3, where o is the measurement outcome. The resulting state us the desired $|\psi_2'\rangle$:

$$|\psi_2'\rangle = \sum_{i,j,k=0}^{2} \omega^{i}\omega^{ij}\omega^{jk}\omega^{2k}\,|k\rangle_{\mathrm{p}_3}|j\rangle_{\mathrm{p}_2}|i\rangle_{\mathrm{p}_1}\ . \tag{23}$$

Similar protocols can be devised to generate the codewords of QECCs associated with any of the AME states discussed in Sec. IV.

VI. PHYSICAL IMPLEMENTATIONS

Photonic qudit states can be generated from a range of different emitters. On the solid-state side, an example is the well-known NV center in diamond, where among its three ground states, $|0\rangle$ and $|\pm 1\rangle$, state $|0\rangle$ can be reliably pumped to an excited state that subsequently decays back down to $|0\rangle$, emitting a photon [77, 78]. NV centers can thus be used to generate photonic time-bin qutrits. Since however the NV has a very low probability of emitting into the zero-phonon line, it may be preferable to consider alternative defects. The silicon-carbon divacancy in SiC is another defect that has a triplet ground state, and that generally resembles the electronic structure of NV-diamond, but with improved optical properties and comparably long coherence times [79]. For local dimension $q = 4$, the silicon vacancy could be used instead.

Atomic systems provide even more options for the value of q, as they can contain well-resolved hyperfine states. Trapped ions such as $^{40}\mathrm{Ca}^{+}$ [80] and $^{171}\mathrm{Yb}^{+}$ [81–83] can serve as multi-level quantum emitters with local dimensions ranging from $q = 3$ up to $q = 7$ [80–85]. There has been significant experimental progress in realizing single- and multi-qudit gate operations in chains of such ions [80, 83]. Few-atom systems in a cavity are another contender for generation of qudit graph states. A recent milestone experiment demonstrated the generation of GHZ and linear cluster states of qubits from a Rb atom [36]. While in that experiment the photonic qubit was encoded in the polarization degree of freedom, and therefore only two of the states in the ground state manifold were used explicitly in the protocol, a similar setup could be employed to demonstrate qudit graph-state generation with time-bin encoding and with more levels participating in generation process (up to $q = 8$ when both the $F = 1$ and the $F = 2$ manifolds are used). To create more complex qudit graphs, cavity-mediated interactions between two or more atoms can be leveraged to create qudit CZ-type gates by modifying the protocol for the already demonstrated two-qubit gates in such systems [86].

VII. CONCLUSIONS AND OUTLOOK

In conclusion, we presented explicit protocols for using coupled, controllable quantum emitters to deterministically generate multi-photon entangled states of time-bin qudits. Although our methods are quite general, we focused primarily on the problem of generating highly entangled states known as AME states, which are important for a number applications in quantum networks and quantum error correction. We showed that such states can be produced from a small number of emitters, with or without photon-emitter interference, provided emitters with the appropriate level structure are available. In some cases, we found that one less emitter can be used if photon-emitter interference is available, providing hints at what sort of resource tradeoffs are possible. Potential candidates include defect centers in solids as well as atomic systems. Our results provide a clear path forward toward the efficient generation of complex states of light for quantum information applications and a guide to experimental groups.

Future directions this work opens include addressing the question of what the minimal resources are—in terms of the number of emitters and the circuit depth—for the generation of a target qudit graph. Similar to the formalism developed to answer these questions in the context of qubits [29], one could set up a similar approach for qudits. Another interesting direction would be to design specific qudit gates for various candidate emitters and to quantify the anticipated performance of the protocols. Our protocols could also be combined with new approaches to photonic one-way quantum repeaters based on photonic qudit states [42] to build error-correction into that approach.

Acknowledgments

We would thank Chenxu Liu and Evangelia Takou for discussions and useful comments. This research is supported by the National Science Foundation (grant nos. 1741656 and 2137953).

[1] Ryszard Horodecki, Paweł Horodecki, Michał Horodecki, and Karol Horodecki. Quantum entanglement. *Rev. Mod. Phys.*, 81:865–942, Jun 2009. doi:10.1103/RevModPhys.81.865. URL `https://link.aps.org/doi/10.1103/RevModPhys.81.865`.

[2] A. J. Scott. Multipartite entanglement, quantum-error-correcting codes, and entangling power of quantum evolutions. *Phys. Rev. A*, 69:052330, May 2004. doi:10.1103/PhysRevA.69.052330. URL `http://link.aps.org/doi/10.1103/PhysRevA.69.052330`.

[3] A. R. Calderbank, E. M. Rains, P. M. Shor, and N. J.A. Sloane. Quantum error correction via codes over gf(4). *IEEE Trans. Inf. Theor.*, 44(4):1369–1387, July 1998. ISSN 0018-9448. doi:10.1109/18.681315. URL `http://dx.doi.org/10.1109/18.681315`.

[4] C. L. Degen, F. Reinhard, and P. Cappellaro. Quantum sensing. *Rev. Mod. Phys.*, 89:035002, Jul 2017. doi:10.1103/RevModPhys.89.035002. URL `https://link.aps.org/doi/10.1103/RevModPhys.89.035002`.

[5] J. I. Cirac, P. Zoller, H. J. Kimble, and H. Mabuchi. Quantum state transfer and entanglement distribution among distant nodes in a quantum network. *Phys. Rev. Lett.*, 78:3221–3224, Apr 1997. doi:10.1103/PhysRevLett.78.3221. URL `https://link.aps.org/doi/10.1103/PhysRevLett.78.3221`.

[6] H. Kimble. The quantum internet. *Nature*, 453:1023–1030, 2008. doi:https://doi.org/10.1038/nature07127. URL `https://www.nature.com/articles/nature07127`.

[7] Mark Hillery, Vladimír Bužek, and André Berthiaume. Quantum secret sharing. *Phys. Rev. A*, 59:1829–1834, Mar 1999. doi:10.1103/PhysRevA.59.1829. URL `https://link.aps.org/doi/10.1103/PhysRevA.59.1829`.

[8] Robert Raussendorf and Hans J. Briegel. A one-way quantum computer. *Phys. Rev. Lett.*, 86:5188–5191, May 2001. doi:10.1103/PhysRevLett.86.5188. URL `https://link.aps.org/doi/10.1103/PhysRevLett.86.5188`.

[9] Sara Bartolucci, Patrick Birchall, Hector Bombin, Hugo Cable, Chris Dawson, Mercedes Gimeno-Segovia, Eric Johnston, Konrad Kieling, Naomi Nickerson, Mihir Pant, Fernando Pastawski, Terry Rudolph, and Chris Sparrow. Fusion-based quantum computation, 2021. URL `https://arxiv.org/abs/2101.09310`.

[10] Srikrishna Omkar, Seok-Hyung Lee, Yong Siah Teo, Seung-Woo Lee, and Hyunseok Jeong. All-photonic architecture for scalable quantum computing with greenberger-horne-zeilinger states. *PRX Quantum*, 3:030309, Jul 2022. doi:10.1103/PRXQuantum.3.030309. URL `https://link.aps.org/doi/10.1103/PRXQuantum.3.030309`.

[11] Nicolas Gisin and Rob Thew. Quantum communication. *Nature Photonics*, 1(3):165–171, 2007. doi:10.1038/nphoton.2007.22. URL `https://doi.org/10.1038/nphoton.2007.22`.

[12] Koji Azuma, Kiyoshi Tamaki, and Hoi-Kwong Lo. All-photonic quantum repeaters. *Nature Communications*, 6 (1):6787, 2015. doi:10.1038/ncomms7787. URL `https://doi.org/10.1038/ncomms7787`.

[13] M. Zwerger, H. J. Briegel, and W. Dür. Measurement-based quantum communication. *Applied Physics B*, 122(3):50, 2016. doi:10.1007/s00340-015-6285-8. URL `https://doi.org/10.1007/s00340-015-6285-8`.

[14] Sreraman Muralidharan, Linshu Li, Jungsang Kim, Norbert Lütkenhaus, Mikhail D. Lukin, and Liang Jiang. Optimal architectures for long distance quantum communication. *Scientific Reports*, 6(1):20463,

2016. doi:10.1038/srep20463. URL https://doi.org/10.1038/srep20463.

[15] T. Guerreiro, A. Martin, B. Sanguinetti, J. S. Pelc, C. Langrock, M. M. Fejer, N. Gisin, H. Zbinden, N. Sangouard, and R. T. Thew. Nonlinear interaction between single photons. *Phys. Rev. Lett.*, 113:173601, Oct 2014. doi:10.1103/PhysRevLett.113.173601. URL https://link.aps.org/doi/10.1103/PhysRevLett.113.173601.

[16] Raymond Knill, Emanuel andLaflamme and Gerald J. Milburn. A scheme for efficient quantum computation with linear optics. *Nature*, 409:46, 2001. doi:https://doi.org/10.1038/35051009. URL https://www.nature.com/articles/3505100.

[17] Pieter Kok, W. J. Munro, Kae Nemoto, T. C. Ralph, Jonathan P. Dowling, and G. J. Milburn. Linear optical quantum computing with photonic qubits. *Rev. Mod. Phys.*, 79:135–174, Jan 2007. doi:10.1103/RevModPhys.79.135. URL https://link.aps.org/doi/10.1103/RevModPhys.79.135.

[18] TP Bodiya and L-M Duan. Scalable generation of graph-state entanglement through realistic linear optics. *Physical review letters*, 97(14):143601, 2006.

[19] Wei-Bo Gao, Chao-Yang Lu, Xing-Can Yao, Ping Xu, Otfried Gühne, Alexander Goebel, Yu-Ao Chen, Cheng-Zhi Peng, Zeng-Bing Chen, and Jian-Wei Pan. Experimental demonstration of a hyper-entangled ten-qubit schrödinger cat state. *Nature Physics*, 6(5):331–335, 2010. doi:10.1038/nphys1603. URL https://doi.org/10.1038/nphys1603.

[20] Jin-Peng Li, Jian Qin, Ang Chen, Zhao-Chen Duan, Ying Yu, YongHeng Huo, Sven Höfling, Chao-Yang Lu, Kai Chen, and Jian-Wei Pan. Multiphoton graph states from a solid-state single-photon source. *ACS Photonics*, 7(7):1603–1610, 07 2020. doi:10.1021/acsphotonics.0c00192. URL https://doi.org/10.1021/acsphotonics.0c00192.

[21] C. Schön, E. Solano, F. Verstraete, J. I. Cirac, and M. M. Wolf. Sequential generation of entangled multiqubit states. *Phys. Rev. Lett.*, 95:110503, Sep 2005. doi:10.1103/PhysRevLett.95.110503. URL https://link.aps.org/doi/10.1103/PhysRevLett.95.110503.

[22] Netanel H. Lindner and Terry Rudolph. Proposal for pulsed on-demand sources of photonic cluster state strings. *Phys. Rev. Lett.*, 103:113602, Sep 2009. doi:10.1103/PhysRevLett.103.113602. URL https://link.aps.org/doi/10.1103/PhysRevLett.103.113602.

[23] Sophia E. Economou, Netanel Lindner, and Terry Rudolph. Optically generated 2-dimensional photonic cluster state from coupled quantum dots. *Phys. Rev. Lett.*, 105:093601, Aug 2010. doi:10.1103/PhysRevLett.105.093601. URL https://link.aps.org/doi/10.1103/PhysRevLett.105.093601.

[24] Donovan Buterakos, Edwin Barnes, and Sophia E. Economou. Deterministic generation of all-photonic quantum repeaters from solid-state emitters. *Phys. Rev. X*, 7:041023, Oct 2017. doi:10.1103/PhysRevX.7.041023. URL https://link.aps.org/doi/10.1103/PhysRevX.7.041023.

[25] Antonio Russo, Edwin Barnes, and Sophia E Economou. Generation of arbitrary all-photonic graph states from quantum emitters. *New Journal of Physics*, 21(5):055002, may 2019. doi:10.1088/1367-2630/ab193d. URL https://doi.org/10.1088/1367-2630/ab193d.

[26] Mercedes Gimeno-Segovia, Terry Rudolph, and Sophia E. Economou. Deterministic generation of large-scale entangled photonic cluster state from interacting solid state emitters. *Phys. Rev. Lett.*, 123:070501, Aug 2019. doi:10.1103/PhysRevLett.123.070501. URL https://link.aps.org/doi/10.1103/PhysRevLett.123.070501.

[27] Paul Hilaire, Edwin Barnes, and Sophia E. Economou. Resource requirements for efficient quantum communication using all-photonic graph states generated from a few matter qubits. *Quantum*, 5:397, February 2021. ISSN 2521-327X. doi:10.22331/q-2021-02-15-397. URL https://doi.org/10.22331/q-2021-02-15-397.

[28] Chenxu Liu, Edwin Barnes, and Sophia Economou. Proposal for generating complex microwave graph states using superconducting circuits, 2022. URL https://arxiv.org/abs/2201.00836.

[29] Bikun Li, Sophia E. Economou, and Edwin Barnes. Photonic resource state generation from a minimal number of quantum emitters. *npj Quantum Information*, 8(1):11, 2022. doi:10.1038/s41534-022-00522-6. URL https://doi.org/10.1038/s41534-022-00522-6.

[30] Howard M. Wiseman and Gerard J. Milburn. *Quantum Measurement and Control*. Cambridge University Press, 2009. doi:10.1017/CBO9780511813948.

[31] Hannes Pichler, Soonwon Choi, Peter Zoller, and Mikhail D. Lukin. Universal photonic quantum computation via time-delayed feedback. *Proceedings of the National Academy of Sciences*, 114(43):11362–11367, 2017. ISSN 0027-8424. doi:10.1073/pnas.1711003114. URL https://www.pnas.org/content/114/43/11362.

[32] Yuan Zhan and Shuo Sun. Deterministic generation of loss-tolerant photonic cluster states with a single quantum emitter. *Phys. Rev. Lett.*, 125:223601, Nov 2020. doi:10.1103/PhysRevLett.125.223601. URL https://link.aps.org/doi/10.1103/PhysRevLett.125.223601.

[33] Yu Shi and Edo Waks. Deterministic generation of multidimensional photonic cluster states using time-delay feedback. *Physical Review A*, 104(1), Jul 2021. ISSN 2469-9934. doi:10.1103/physreva.104.013703. URL http://dx.doi.org/10.1103/PhysRevA.104.013703.

[34] I. Schwartz, D. Cogan, E. R. Schmidgall, Y. Don, L. Gantz, O. Kenneth, N. H. Lindner, and D. Gershoni. Deterministic generation of a cluster state of entangled photons. *Science*, 354(6311):434–437, 2016. doi:10.1126/science.aah4758. URL https://www.science.org/doi/abs/10.1126/science.aah4758.

[35] Jean-Claude Besse, Kevin Reuer, Michele C. Collodo, Arne Wulff, Lucien Wernli, Adrian Copetudo, Daniel Malz, Paul Magnard, Abdulkadir Akin, Mihai Gabureac, Graham J. Norris, J. Ignacio Cirac, Andreas Wallraff, and Christopher Eichler. Realizing a deterministic source of multipartite-entangled photonic qubits. *Nature Communications*, 11(1):4877, Sep 2020. ISSN 2041-1723. doi:10.1038/s41467-020-18635-x. URL https://doi.org/10.1038/s41467-020-18635-x.

[36] Philip Thomas, Leonardo Ruscio, Olivier Morin, and Gerhard Rempe. Efficient generation of entangled multiphoton graph states from a single atom. *Nature*, 608 (7924):677–681, 2022. doi:10.1038/s41586-022-04987-5. URL https://doi.org/10.1038/s41586-022-04987-5.

[37] N. Coste, D. Fioretto, N. Belabas, S. C. Wein, P. Hilaire, R. Frantzeskakis, M. Gundin, B. Goes, N. Somaschi, M. Morassi, A. Lemaître, 1 I. Sagnes, A. Harouri, S. E. Economou, A. Auffeves, O. Krebs, L. Lanco, and

P. Senellart. High-rate entanglement between a semiconductor spin and indistinguishable photons, 2022. URL https://arxiv.org/abs/2207.09881.

[38] Michael Kues, Christian Reimer, Piotr Roztocki, Luis Romero Cortés, Stefania Sciara, Benjamin Wetzel, Yanbing Zhang, Alfonso Cino, Sai T. Chu, Brent E. Little, David J. Moss, Lucia Caspani, José Azana, and Roberto Morandotti. On-chip generation of high-dimensional entangled quantum states and their coherent control. *Nature*, 546:622, 2017. doi:https://doi.org/10.1038/nature22986. URL https://www.nature.com/articles/nature22986.

[39] Manuel Erhard, Mario Krenn, and Anton Zeilinger. Advances in high-dimensional quantum entanglement. *Nature*, 2:365, 2020. doi:https://doi.org/10.1038/s42254-020-0193-5. URL https://www.nature.com/articles/s42254-020-0193-5.

[40] Yuchen Wang, Zixuan Hu, Barry C. Sanders, and Sabre Kais. Qudits and high-dimensional quantum computing. *Frontiers in Physics*, 8, 2020. ISSN 2296-424X. doi:10.3389/fphy.2020.589504. URL https://www.frontiersin.org/articles/10.3389/fphy.2020.589504.

[41] Sreraman Muralidharan, Chang-Ling Zou, Linshu Li, and Liang Jiang. One-way quantum repeaters with quantum reed-solomon codes. *Phys. Rev. A*, 97:052316, May 2018. doi:10.1103/PhysRevA.97.052316. URL https://link.aps.org/doi/10.1103/PhysRevA.97.052316.

[42] Yunzhe Zheng, Hemant Sharma, and Johannes Borregaard. Entanglement distribution with minimal memory requirements using time-bin photonic qudits. *PRX Quantum*, 3(4), nov 2022. doi:10.1103/prxquantum.3.040319. URL https://doi.org/10.1103%2Fprxquantum.3.040319.

[43] Christian Reimer, Stefania Sciara, Piotr Roztocki, Mehedi Islam, Luis Romero Cortés, Yanbing Zhang, Bennet Fischer, Sébastien Loranger, Raman Kashyap, Alfonso Cino, Sai T. Chu, Brent E. Little, David J. Moss, Lucia Caspani, William J. Munro, José Azaña, Michael Kues, and Roberto Morandotti. High-dimensional one-way quantum processing implemented on d-level cluster states. *Nature Physics*, 15(2):148–153, 2019. doi:10.1038/s41567-018-0347-x. URL https://doi.org/10.1038/s41567-018-0347-x.

[44] Wolfram Helwig, Wei Cui, José Ignacio Latorre, Arnau Riera, and Hoi-Kwong Lo. Absolute maximal entanglement and quantum secret sharing. *Phys. Rev. A*, 86:052335, Nov 2012. doi:10.1103/PhysRevA.86.052335. URL http://link.aps.org/doi/10.1103/PhysRevA.86.052335.

[45] W. Helwig and W. Cui. Absolutely maximally entangled states: Existence and applications. 2013. URL https://arxiv.org/abs/1306.2536.

[46] Zahra Raissi, Christian Gogolin, Arnau Riera, and Antonio Acín. Optimal quantum error correcting codes from absolutely maximally entangled states. *Journal of Physics A: Mathematical and Theoretical*, 51(7):075301, jan 2018. doi:10.1088/1751-8121/aaa151. URL https://doi.org/10.1088/1751-8121/aaa151.

[47] Dardo Goyeneche, Zahra Raissi, Sara Di Martino, and Karol Życzkowski. Entanglement and quantum combinatorial designs. *Phys. Rev. A*, 97:062326, Jun 2018. doi:10.1103/PhysRevA.97.062326. URL https://link.aps.org/doi/10.1103/PhysRevA.97.062326.

[48] Zahra Raissi, Adam Teixidó, Christian Gogolin, and Antonio Acín. Constructions of k-uniform and absolutely maximally entangled states beyond maximum distance codes. *Phys. Rev. Research*, 2:033411, Sep 2020. doi:10.1103/PhysRevResearch.2.033411. URL https://link.aps.org/doi/10.1103/PhysRevResearch.2.033411.

[49] Zahra Raissi. Modifying method of constructing quantum codes from highly entangled states. *IEEE Access*, 8:222439–222448, 2020. doi:10.1109/ACCESS.2020.3043401.

[50] Zahra Raissi, Adam Burchardt, and Edwin Barnes. General stabilizer approach for constructing highly entangled graph states. 2021. URL https://arxiv.org/abs/2111.08045.

[51] M. Hein, W. Dür, J. Eisert, R. Raussendorf, M. Van den Nest, and H. J Briegel. Entanglement in graph states and its applications. 2006. URL https://arxiv.org/abs/quant-ph/0602096.

[52] Maarten Van den Nest, Jeroen Dehaene, and Bart De Moor. Graphical description of the action of local clifford transformations on graph states. *Phys. Rev. A*, 69:022316, Feb 2004. doi:10.1103/PhysRevA.69.022316. URL https://link.aps.org/doi/10.1103/PhysRevA.69.022316.

[53] M. Hein, J. Eisert, and H. J. Briegel. Multiparty entanglement in graph states. *Phys. Rev. A*, 69:062311, June 2004. doi:10.1103/PhysRevA.69.062311.

[54] M. Bahramgiri and S. Beigi. Graph states under the action of local clifford group in non-binary case. 2006. URL https://arxiv.org/abs/quant-ph/0610267.

[55] Robert Raussendorf and Hans J. Briegel. A one-way quantum computer. *Phys. Rev. Lett.*, 86:5188–5191, May 2001. doi:10.1103/PhysRevLett.86.5188. URL https://link.aps.org/doi/10.1103/PhysRevLett.86.5188.

[56] D. Gottesman. *Stabilizer codes and quantum error correction*. PhD thesis, Caltech, 1997. URL https://arxiv.org/abs/quant-ph/9705052.

[57] D. Gottesman. An introduction to quantum error correction and fault-tolerant quantum computation. 2009. URL http://www.arXiv.org/abs/0904.2557.

[58] Netanel H. Lindner and Terry Rudolph. Proposal for pulsed on-demand sources of photonic cluster state strings. *Phys. Rev. Lett.*, 103:113602, Sep 2009. doi:10.1103/PhysRevLett.103.113602. URL https://link.aps.org/doi/10.1103/PhysRevLett.103.113602.

[59] J P Lee, B Villa, A J Bennett, R M Stevenson, D J P Ellis, I Farrer, D A Ritchie, and A J Shields. A quantum dot as a source of time-bin entangled multi-photon states. *Quantum Science and Technology*, 4(2):025011, mar 2019. doi:10.1088/2058-9565/ab0a9b. URL https://doi.org/10.1088/2058-9565/ab0a9b.

[60] Paolo Facchi. Multipartite entanglement in qubit systems. *Atti Accad. Naz. Lincei Cl. Sci. Fis. Mat. Natur.*, 20:25, 2009. doi:DOI 10.4171/RLM/532. URL https://ems.press/journals/rlm/articles/1988.

[61] Dardo Goyeneche, Daniel Alsina, José I. Latorre, Arnau Riera, and Karol Życzkowski. Absolutely maximally entangled states, combinatorial designs, and multiunitary matrices. *Phys. Rev. A*, 92:032316, Sep 2015. doi:10.1103/PhysRevA.92.032316. URL https://link.aps.org/doi/10.1103/PhysRevA.92.032316.

[62] Z. Raissi and V. Karimipour. Creating maximally entangled states by gluing. *Quantum Inf Process*, 16:81, 2017. doi:https://doi.org/10.1007/s11128-017-1535-9.

[63] E. M. Rains. Quantum shadow enumerators. *IEEE Transactions on Information Theory*, 45(6418557):2361 – 2366, 1999. doi:10.1109/18.796376. URL http://ieeexplore.ieee.org/document/796376/.

[64] W. Helwig. Absolutely maximally entangled qudit graph states. 2013. URL https://arxiv.org/abs/1306.2879.

[65] Sophia E. Economou, Netanel Lindner, and Terry Rudolph. Optically generated 2-dimensional photonic cluster state from coupled quantum dots. *Phys. Rev. Lett.*, 105:093601, Aug 2010. doi:10.1103/PhysRevLett.105.093601. URL https://link.aps.org/doi/10.1103/PhysRevLett.105.093601.

[66] Antonio Russo, Edwin Barnes, and Sophia E Economou. Generation of arbitrary all-photonic graph states from quantum emitters. *New Journal of Physics*, 21(5):055002, may 2019. doi:10.1088/1367-2630/ab193d. URL https://doi.org/10.1088/1367-2630/ab193d.

[67] Mercedes Gimeno-Segovia, Terry Rudolph, and Sophia E. Economou. Deterministic generation of large-scale entangled photonic cluster state from interacting solid state emitters. *Phys. Rev. Lett.*, 123:070501, Aug 2019. doi:10.1103/PhysRevLett.123.070501. URL https://link.aps.org/doi/10.1103/PhysRevLett.123.070501.

[68] Cathryn P. Michaels, Jesús Arjona Martínez, Romain Debroux, Ryan A. Parker, Alexander M. Stramma, Luca I. Huber, Carola M. Purser, Mete Atatüre, and Dorian A. Gangloff. Multidimensional cluster states using a single spin-photon interface coupled strongly to an intrinsic nuclear register. *Quantum*, 5:565, October 2021. ISSN 2521-327X. doi:10.22331/q-2021-10-19-565. URL https://doi.org/10.22331/q-2021-10-19-565.

[69] R. Laflamme, C. Miquel, J. P. Paz, and W. Zurek. Perfect quantum error correcting code. *Physical Review Lett.*, 77 (198), 1996. ISSN 1079-7114. URL https://doi.org/10.1103/PhysRevLett.77.198.

[70] Kianna Wan, Soonwon Choi, Isaac H. Kim, Noah Shutty, and Patrick Hayden. Fault-tolerant qubit from a constant number of components. *PRX Quantum*, 2:040345, Dec 2021. doi:10.1103/PRXQuantum.2.040345. URL https://link.aps.org/doi/10.1103/PRXQuantum.2.040345.

[71] Yu Shi and Edo Waks. Deterministic generation of multidimensional photonic cluster states using time-delay feedback. *Phys. Rev. A*, 104:013703, Jul 2021. doi:10.1103/PhysRevA.104.013703. URL https://link.aps.org/doi/10.1103/PhysRevA.104.013703.

[72] Alba Cervera-Lierta, José Ignacio Latorre, and Dardo Goyeneche. Quantum circuits for maximally entangled states. *Phys. Rev. A*, 100:022342, Aug 2019. doi:10.1103/PhysRevA.100.022342. URL https://link.aps.org/doi/10.1103/PhysRevA.100.022342.

[73] Felix Huber, Otfried Gühne, and Jens Siewert. Absolutely maximally entangled states of seven qubits do not exist. *Phys. Rev. Lett.*, 118:200502, May 2017. doi:10.1103/PhysRevLett.118.200502. URL https://link.aps.org/doi/10.1103/PhysRevLett.118.200502.

[74] Emanuel Knill and Raymond Laflamme. Theory of quantum error-correcting codes. *Phys. Rev. A*, 55:900–911, Feb 1997. doi:10.1103/PhysRevA.55.900. URL http://link.aps.org/doi/10.1103/PhysRevA.55.900.

[75] A. Ketkar, A. Klappenecker, S. Kumar, and P. K. Sarvepalli. Nonbinary stabilizer codes over finite fields. *IEEE Transactions on Information Theory*, 52(11):4892–4914, Nov 2006. ISSN 0018-9448. doi:10.1109/TIT.2006.883612. URL http://ieeexplore.ieee.org/document/1715533/.

[76] Daniel Alsina and Mohsen Razavi. Absolutely maximally entangled states, quantum-maximum-distance-separable codes, and quantum repeaters. *Phys. Rev. A*, 103: 022402, Feb 2021. doi:10.1103/PhysRevA.103.022402. URL https://link.aps.org/doi/10.1103/PhysRevA.103.022402.

[77] Marcus W. Doherty, Neil B. Manson, Paul Delaney, Fedor Jelezko, Jörg Wrachtrup, and Lloyd C.L. Hollenberg. The nitrogen-vacancy colour centre in diamond. *Physics Reports*, 528(1):1–45, 2013. ISSN 0370-1573. doi:https://doi.org/10.1016/j.physrep.2013.02.001. URL https://www.sciencedirect.com/science/article/pii/S0370157313000562. The nitrogen-vacancy colour centre in diamond.

[78] Gary Wolfowicz, F. Joseph Heremans, Christopher P. Anderson, Shun Kanai, Hosung Seo, Adam Gali, Giulia Galli, and David D. Awschalom. Quantum guidelines for solid-state spin defects. *Nature Reviews Materials*, 6(10): 906–925, 2021. doi:10.1038/s41578-021-00306-y. URL https://doi.org/10.1038/s41578-021-00306-y.

[79] David J. Christle, Abram L. Falk, Paolo Andrich, Paul V. Klimov, Jawad Ul Hassan, Nguyen T. Son, Erik Janzén, Takeshi Ohshima, and David D. Awschalom. Isolated electron spins in silicon carbide with millisecond coherence times. *Nature Materials*, 14(2):160–163, 2015. doi:10.1038/nmat4144. URL https://doi.org/10.1038/nmat4144.

[80] M. Ringbauer, M. Meth, L. Postler, R. Stricker, R. Blatt, P. Schindler, and T. Monz. A universal qudit quantum processor with trapped ions. *Nature Physics*, (18): 1053–1057, 2022.

[81] N. Timoney, I. Baumgart, M. Johanning, Varón A. F., Plenio M. B., Retzker A., and Wunderlich Ch. Quantum gates and memory using microwave-dressed states. *Nature*, 476:185–188, 2011. doi:https://doi.org/10.1038/nature10319. URL https://www.nature.com/articles/nature10319.

[82] S. C. Webster, S. Weidt, K. Lake, J. J. McLoughlin, and W. K. Hensinger. Simple manipulation of a microwave dressed-state ion qubit. *Phys. Rev. Lett.*, 111:140501, Oct 2013. doi:10.1103/PhysRevLett.111.140501. URL https://link.aps.org/doi/10.1103/PhysRevLett.111.140501.

[83] M.A. Aksenov, I.V. Zalivako, I.A. Semerikov, A.S. Borisenko, N.V. Semenin, P.L. Sidorov, A.K. Fedorov, K.Yu. Khabarova, and N.N. Kolachevsky. Realizing quantum gates with optically-addressable 171yb+ ion qudits, 2022. URL https://arxiv.org/abs/2210.09121.

[84] J. Randall, S. Weidt, E. D. Standing, K. Lake, S. C. Webster, D. F. Murgia, T. Navickas, K. Roth, and W. K. Hensinger. Efficient preparation and detection of microwave dressed-state qubits and qutrits with trapped ions. *Phys. Rev. A*, 91:012322, Jan 2015. doi:10.1103/PhysRevA.91.012322. URL https://link.aps.org/doi/10.1103/PhysRevA.91.012322.

[85] C. Senko, P. Richerme, J. Smith, A. Lee, I. Cohen, A. Retzker, and C. Monroe. Realization of a quantum integer-spin chain with controllable interactions. *Phys. Rev. X*, 5:021026, Jun 2015.

doi:10.1103/PhysRevX.5.021026. URL https://link.aps.org/doi/10.1103/PhysRevX.5.021026.

[86] Stephan Welte, Bastian Hacker, Severin Daiss, Stephan Ritter, and Gerhard Rempe. Photon-mediated quantum gate between two neutral atoms in an optical cavity. *Phys. Rev. X*, 8:011018, Feb 2018. doi:10.1103/PhysRevX.8.011018. URL https://link.aps.org/doi/10.1103/PhysRevX.8.011018.